

Time dependent behavior of piled raft foundation in clayey soil

Mohammed Y. Fattah*¹, Mosa J. Al-Mosawi² and Abbas A.O. Al-Zayadi²

¹*Building and Construction Engineering Department, University of Technology, Iraq*

²*College of Engineering, Civil Engineering Department, University of Baghdad, Iraq*

(Received February 25, 2012, Revised October 6, 2012, Accepted October 6, 2012)

Abstract. Settlement of the piled raft can be estimated even after years of completing the construction of any structure over the foundation. This study is devoted to carry out numerical analysis by the finite element method of the consolidation settlement of piled rafts over clayey soils and detecting the dissipation of excess pore water pressure and its effect on bearing capacity of piled raft foundations. The ABAQUS computer program is used as a finite element tool and the soil is represented by the modified Drucker-Prager/cap model. Five different configurations of pile groups are simulated in the finite element analysis.

It was found that the settlement beneath the piled raft foundation resulted from the dissipation of excess pore water pressure considerably affects the final settlement of the foundation, and enough attention should be paid to settlement variation with time. The settlement behavior of unpiled raft shows bowl shaped settlement profile with maximum at the center. The degree of curvature of the raft under vertical load increases with the decrease of the raft thickness. For the same vertical load, the differential settlement of raft of (10x10 m) size decreases by more than 90% when the raft thickness increased from 0.75 m to 1.5 m. The average load carried by piles depends on the number of piles in the group. The groups of (2x1, 3x1, 2x2, 3x2, and 3x3) piles were found to carry about 24%, 32%, 42%, 58%, and 79% of the total vertical load. The distribution of load between piles becomes more uniform with the increase of raft thickness.

Keywords: piled raft; foundation; finite elements; time; clay

1. Introduction

The use of piled raft foundations has become more popular in the recent years, as the combined action of the raft and the piles can increase the bearing capacity, reduce settlement, and the piles can be arranged so as to reduce differential deflection in the raft. Many authors have been attracted to piled raft foundation; early researches focused on hand calculations techniques with the help of empirical charts and formulas for single pile and pile groups. With the advent of the computers and numerical procedures, finite element techniques were developed to solve piled foundation, whereas most of the piled raft problems today can be solved with microcomputers.

Piled raft foundations are composite structures unlike classical foundation where the building load is either transferred by the raft or the piles alone. In a piled raft foundation, the contribution of the piles as well as the raft is taken into account. The piles transfer a part of the building loads into deeper and stiffer layers of soil and thereby allow the reduction of settlement and differential settlement in a very economic way. Piles are used up to a load level which can be of the same

*Corresponding author, Professor, E-mail: myf_1968@yahoo.com

order of magnitude as the bearing capacity of a comparable single pile or even greater.

2. Types of piled raft foundations

On the basis of the design requirements to be satisfied, Russo and Viggiani (1998) grouped piled rafts into two broad categories:

- I. Small piled rafts; i.e., those in which the bearing capacity of the unpiled raft is insufficient, and thus the primary reason to add the piles is to achieve a suitable safety factor. The width of the raft B_r , belonging to this category, is generally small in comparison to the length L of the piles ($B_r/L < 1$) and amounts to a few meters. The flexural stiffness of the raft is usually high and the differential settlement does not represent a problem.
- II. Large piled rafts; i.e., those in which the bearing capacity is sufficient to carry the total load with a reasonable margin, so that the addition of piles is usually intended to reduce settlement. In general, the width B_r of the raft is relatively large in comparison with the length of the piles ($B_r/L > 1$).

The problem of bearing capacity failure is of particular concern for the *small* piled rafts, and for the case of soft clay soils.

3. Time dependent behavior of piled raft foundation

Applying load to saturated soft soil layers by structures such as buildings causes the development of excess pore water pressure. Initially, the structure will undergo an immediate settlement as the excess pore pressure develops. However, with time, the excess pore pressure will dissipate as water flows from regions of high excess pore water pressure to regions of lower water pressure. As the excess pore pressure decreases, the effective stresses in the soil increase progressively, and this leads to further settlement of the foundation with time.

Analysis of structures on consolidating soils has been limited in the past because of the complexity of the time dependent interaction between the soil and the structure. Some solutions are available for the consolidation of a circular raft on a porous elastic soil and for a pile group treated as a solid block, but these solutions are limited in their scope and application (Small and Liu 2008).

Although there has been a great deal of attention paid to the settlement of pile groups and piled raft foundations, little attention has been paid to the time- dependent behavior. Therefore, this study will be directed to the analysis of piled raft system over consolidating soils.

In the design of piled raft, design engineers have to understand the mechanism of load transfer from the raft to the piles and to the soil to predict (Chow 2007):

1. The behavior of raft which include the settlement, bending moment and the proportion of load carried by the raft.
2. The behavior of piles which includes the displacement and load distribution along the piles.
3. Interaction between piles, raft and soil are of major concern in the analysis.

The objective of this study is to carry out numerical solution by the finite element method. The



Fig. 1 Three dimensional view of the piled raft configurations adopted in the finite element study

problem takes the effect of time into consideration through the studying of consolidation of clayey soils and detecting the dissipation of excess pore water pressure and its effect on bearing capacity of the foundation. Settlement of the piled raft can be estimated even after years of completing the construction of any structure over a piled raft foundation.

4. Description of the Piled Raft Problem

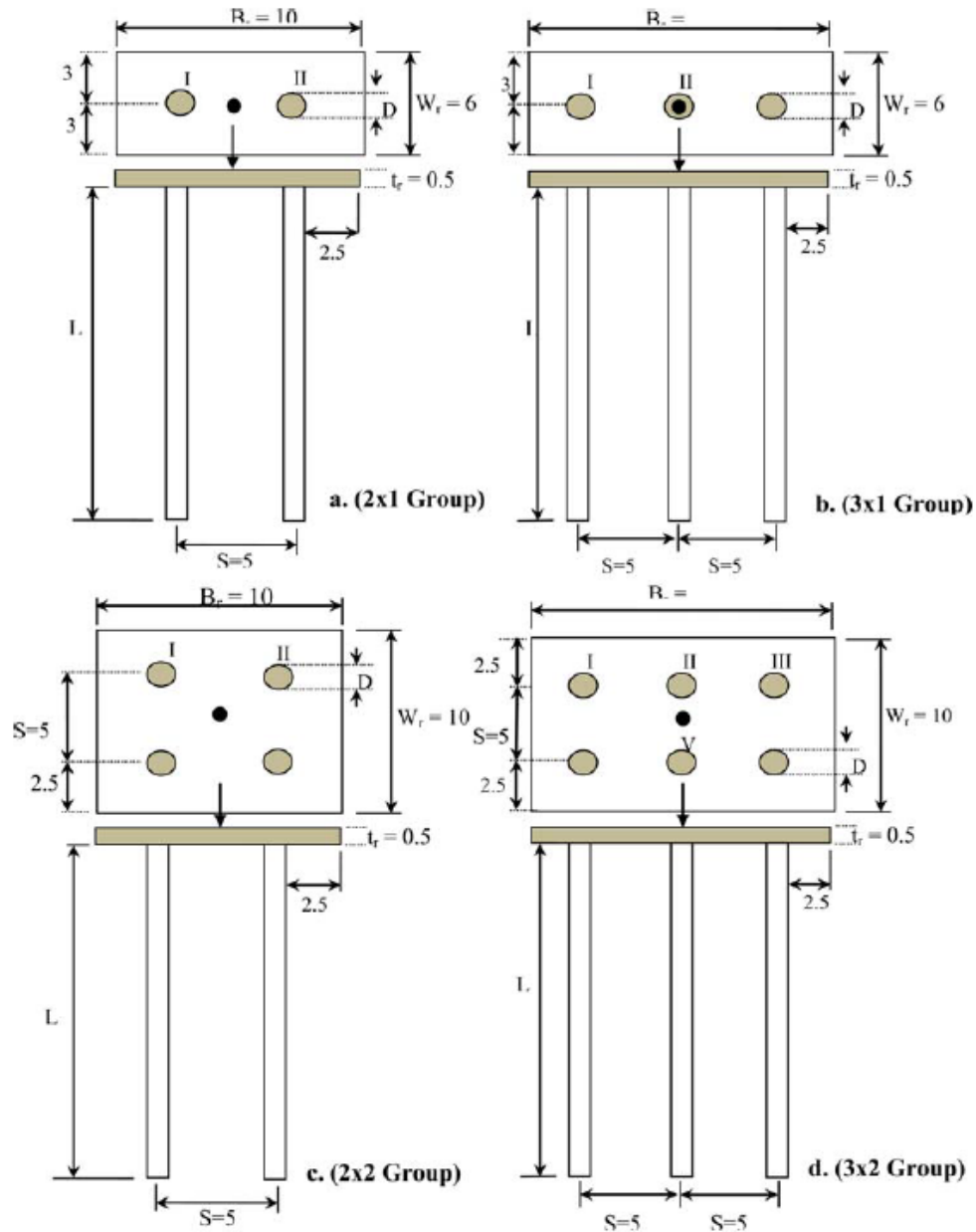
Using a raft alone as a foundation results in excessive settlement and the use of pile groups is too costly, a piled raft is a feasible solution. The use of a piled raft as the foundation for building has proven to be an effective and economical way to control the total settlement as well as bearing capacity.

The performance of a piled raft can be influenced by several factors such as the condition of the supporting soil, loading condition, size and length of the piles, pile arrangement, and other factors. Regarding the soil situation, the permeability has significant effect on the rate of dissipation of pore water pressure, and therefore affects the consolidation settlement.

In this study, the pile groups are constructed in clayey soil with the existence of pore water pressure. The ABAQUS computer program is used as a finite element tool and the soil is represented by the modified Drucker-Prager/cap model.

Five different configurations of pile groups are simulated in the finite element analysis. Fig. 1 shows a three dimensional view for the five configurations of the piled groups, while the plan view for four of the groups is shown in Fig. 2.

In the finite element solution, the circular cross section of piles is replaced with square ones with the same equivalent area, and both the soil and piled raft systems are meshed with the 8-nodes brick elements, whereas the pore water pressure is allowed for soil and not allowed through the piled raft. In the program ABAQUS, it is important to mesh the interacted surface with



*Note: All dimensions are in meters.

Fig. 2 Three dimensional view of the piled raft configurations adopted in the finite element study

the same type and size of the element, since the interaction is simulated through defining surfaces with contact properties (as the case of pile-soil interaction and raft-soil interaction).

As shown in Fig. 1, the five configurations of pile are arranged symmetrically, though in the finite element solution, only quarter of the problem can be used to represent the whole problem keeping the necessary computer time as minimum as possible. Boundary conditions are used to

simulate the axes of symmetry, where displacement normal to the axis of symmetry is set zero. The lateral boundaries of the soil are chosen to be far enough from the zone of influence under the vertical load, the lower boundary simulating the depth of the soil layer is also kept far enough from the pile bottom as the piles are assumed to be floated piles (i.e. the piles are not driven to a rigid stratum). Even though the vertical displacement at the lateral and vertical boundary is zero, a boundary condition prescribing the vertical displacement with a value of zero is considered. The pore water pressure is assumed to remain zero at the upper boundary, therefore one way drainage is occurring.

The piled raft foundation material is assumed to be linear elastic having the following properties:

$$\begin{aligned} \text{Young's modulus of elasticity } E_r &= 20 \times 10^6 \text{ kN/m}^2, \text{ and} \\ \text{Poisson's ratio } \nu_r &= 0.3 \end{aligned}$$

The clayey soil is modeled as homogeneous isotropic elasto-plastic soil following the modified Drucker-Prager/cap constitutive relation. The properties of the soil considered in this study represent part of Baghdad soil, according to Al-Saady (1989) who tested compacted clay samples. The results of Al-Saady tests are used to calculate the effective strength parameters of Drucker-Prager constitutive model, the parameters are listed below:

| | |
|---|--|
| Young's modulus of elasticity, E_s | $1.22 \times 10^4 \text{ kN/m}^2$ |
| Effective Poisson's ratio, ν_s | 0.20 |
| Effective cohesion, c' | 0 |
| Effective angle of internal friction, ϕ' | 38° |
| Permeability, k | $1 \times 10^{-7} \text{ m/sec (0.259 m/month)}$ |

5. Time dependent behavior of the unpiled raft

Before testing the piled raft model, unpiled rafts with the sizes of (15×15, 10×15, 10×10, 6×15, and 6×10) m are analyzed; the settlement at the center of the raft is investigated with time.

By reviewing the literature, it was found that for expressing the load settlement behavior under piled and unpiled rafts under vertical concentrated load, dimensionless factors are used as follows

$$I_d = \frac{Pt_r}{u_z E_s BW} \quad (1)$$

where

| | |
|-------|---|
| P | = Applied vertical load, |
| u_z | = Displacement at the center of the raft, |
| E_s | = Soil modulus of elasticity, |
| B | = Length of the unpiled raft, |
| W | = Width of the unpiled raft, and |
| t_r | = Thickness of the unpiled raft. |

Unpiled raft is simulated in the finite element program ABAQUS in its full size, with dimensions of ($B \times W$). The behavior of the clay with time is expressed in terms of pore water

pressure which is generated after applying the load.

A block of modeled soil with dimensions of (6W * 6B * 8B) is used in the finite element solution, these dimensions are chosen to be far enough from the zone of influence, biased meshing techniques is used to discretize the soil, where finer meshes are used near the raft as the concentration of vertical stress and displacement is expected to occur.

A vertical load of 10000 kN is applied in a short time simulating the gradual loading to the unpiled rafts of the five different dimensions. The load is concentrated in the middle of the raft. The settlement under the raft is calculated at different times, where time is introduced through the dimensionless time factor defined in Eq. (2), this factor can be written in the following term (Small and Liu 2008)

$$T_v = \frac{k(1-\nu_s)E_s t}{\gamma_w(1-2\nu_s)(1+\nu_s)(H)^2} \quad (2)$$

where, t is the time,

γ_w is the unit weight of water,

k is the coefficient of permeability, and

H is the thickness of the clay layer which represents the drainage path, the raft is considered as impermeable footing.

Figs. 3 to 8 show a contour mapping and two dimensional plots of the variation of pore pressure with time under the unpiled rafts of thickness 1.0 m and sizes of (15×15, 10×15, 10×10, 6×15, and 6×10) m, respectively. The maximum pore water pressure is noticed to be at the end of load application step (0.1 month). After 0.5 month of applying the load, the rate of pore water pressure dissipation is noticed to be the maximum, the pore water pressure needs about 50 months to become of negligible value. For the case of (6×10 m) raft, the pore water pressure dose not approach zero even after 50 months, this may be attributed to that the area of the raft is relatively small which lead to generation of high vertical stress due to the applied load.

A section passing through the center of the unpiled raft is made to observe the vertical settlement at different time factors. Figs. 9 to 13 show the normalized settlement of the soil under the unpiled raft at different time factors for the set of five cases, respectively.

These figures indicate that the settlement may occur at the loading step and only a small fraction may result from the dissipation of excess pore water pressure, except the case of (6×10); the smallest size of unpiled raft, where the raft takes the shape of widely open bowel, whereas the difference between the settlements of the center and edges is of big value. This may be attributed to that the geometry of the raft is relatively smaller than the other rafts.

For the other case, it seems that the soil does not reach the plastic range, therefore the deformation shape of the unpiled raft is concaved downward in the direction of the applied load, and the differential settlement is remarkably noticed as shown in figures. The settlement at the center of unpiled raft with rectangular shape of (15×6 m) and (15×10 m) is about 45% and 38% respectively greater than the settlement at the edges of the raft. The settlement at the center for unpiled raft of square shape of (10×10 m) and (15×15 m) is about 25% and 28% respectively greater than the settlement at the edges of the raft.

To study the effect of unpiled raft thickness on the vertical stresses and settlement, the case of (10×10) raft size is considered with four thicknesses of (0.75, 1.00, 1.25, and 1.5 m). Fig. 14 shows the variation of vertical stress under the center of the raft with time factor, while Fig. 15 shows the normalized settlement along the raft with different thicknesses. The effect is more

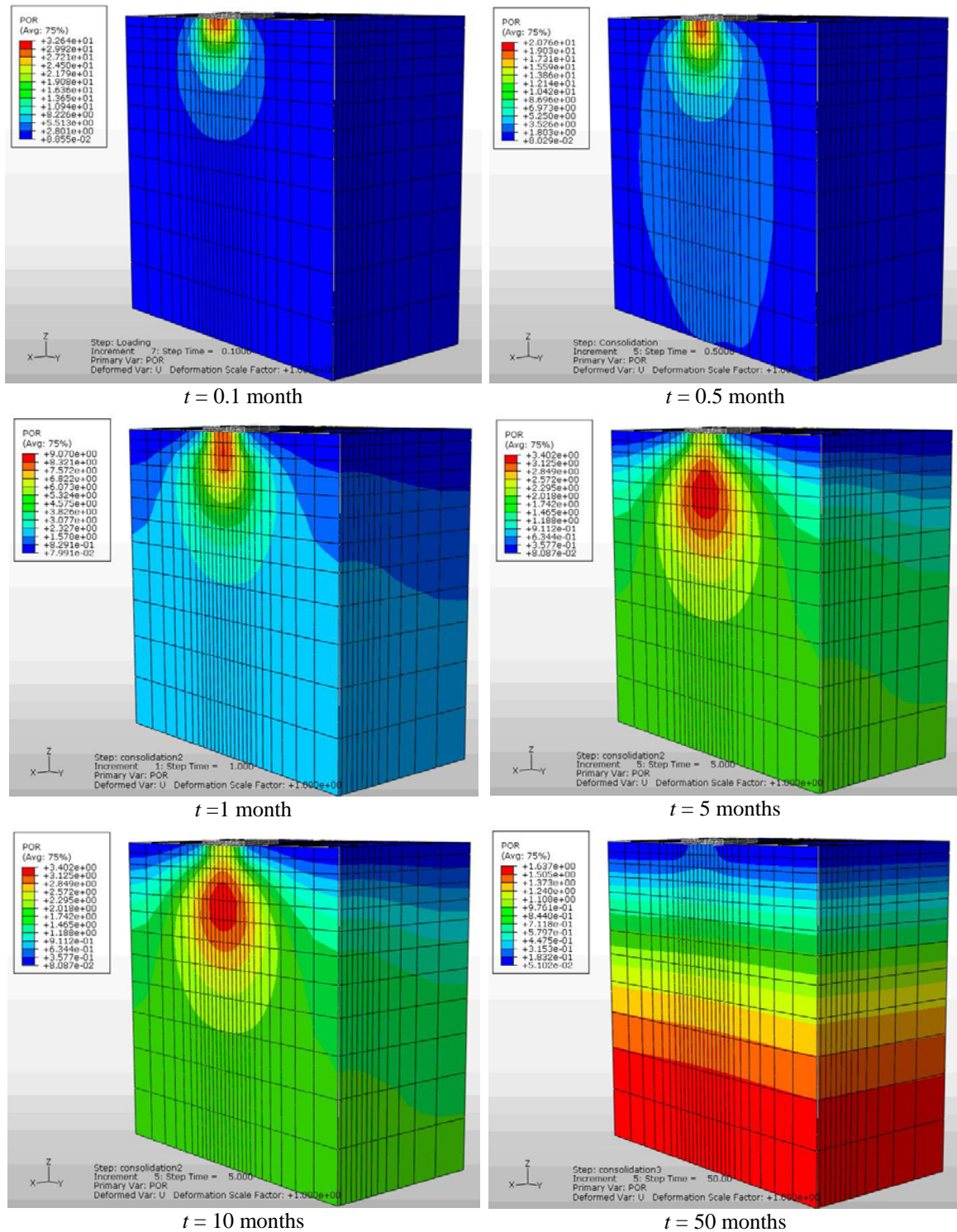
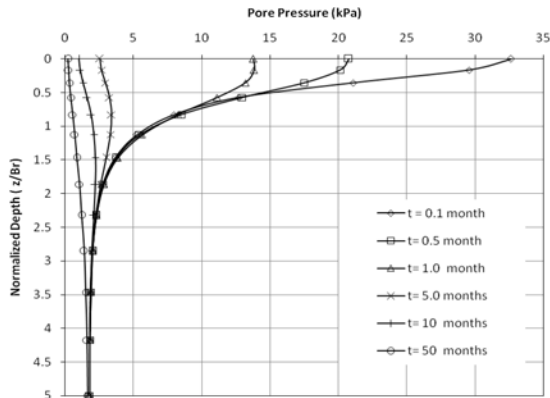
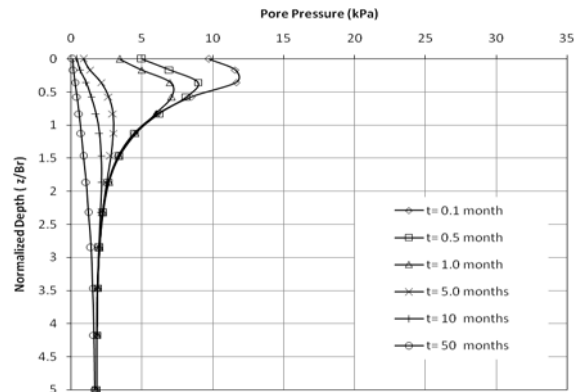


Fig. 3 Three dimensional contour mapping of pore water pressure (kPa) at different times, raft size (15×15) m

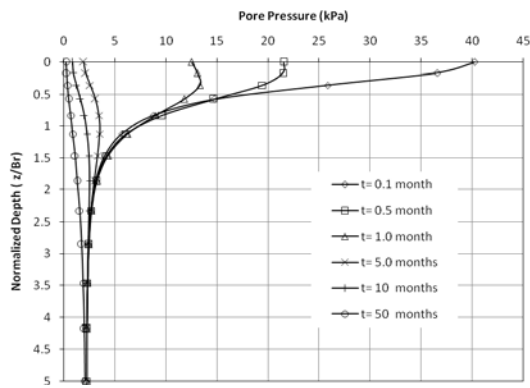


(a) Pore water pressure below the raft center at different times

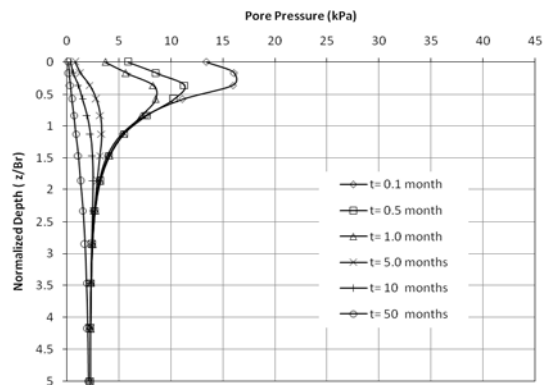


(b) Pore water pressure below the raft edge at different times

Fig. 4 Variation of pore water pressure beneath unpiled raft of (15×15) m size

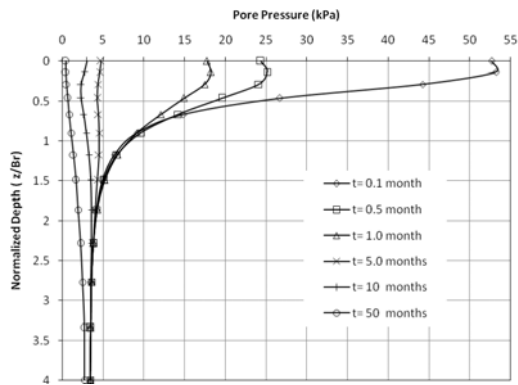


(a) Pore water pressure below the raft center at different times

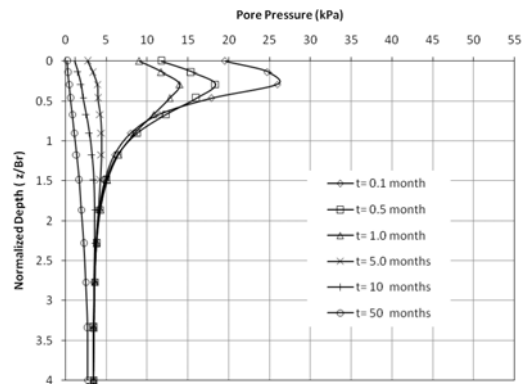


(b) Pore water pressure below the raft edge at different times

Fig. 5 Variation of pore water pressure beneath unpiled raft of (10×15) m size

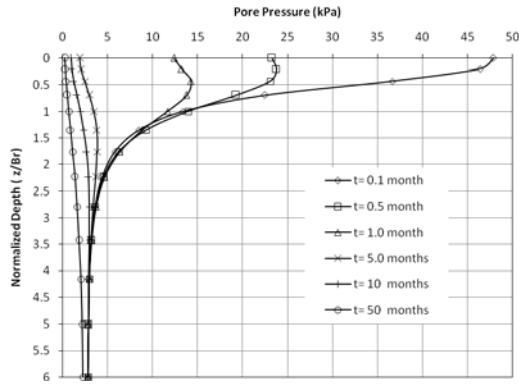


(a) Pore water pressure below the raft center at different times

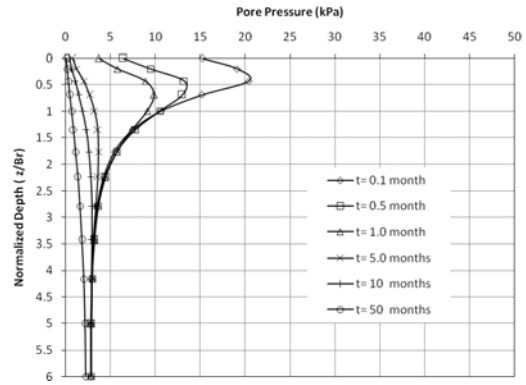


(b) Pore water pressure below the raft edge at different times

Fig. 6 Variation of pore water pressure beneath unpiled raft of (6×15) m size

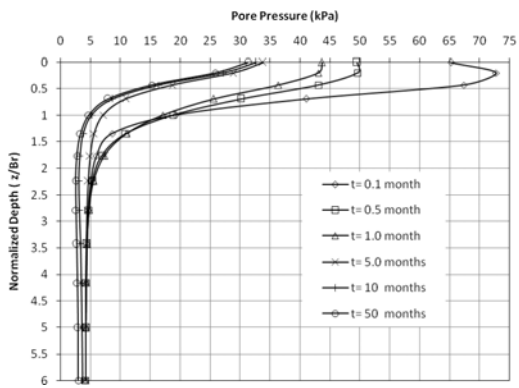


(a) Pore water pressure below the raft center at different times

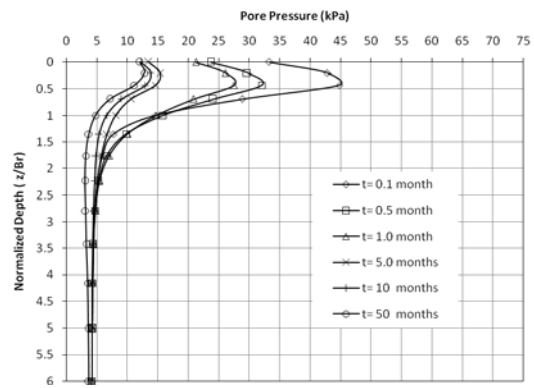


(b) Pore water pressure below the raft edge at different times

Fig. 7 Variation of pore water pressure beneath unpiled raft of (10x10) m size



(a) Pore water pressure below the raft center at different times



(b) Pore water pressure below the raft edge at different times

Fig. 8 Variation of pore water pressure beneath unpiled raft of (6x10) m size

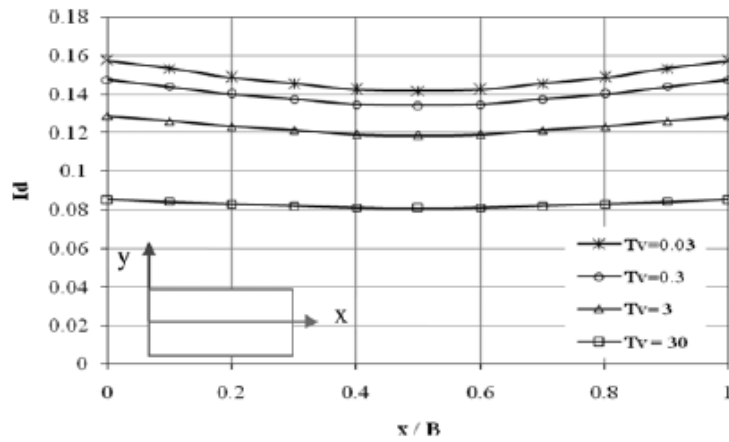


Fig. 9 Normalized vertical displacement under unpiled raft of (6x10) m size at different time factors

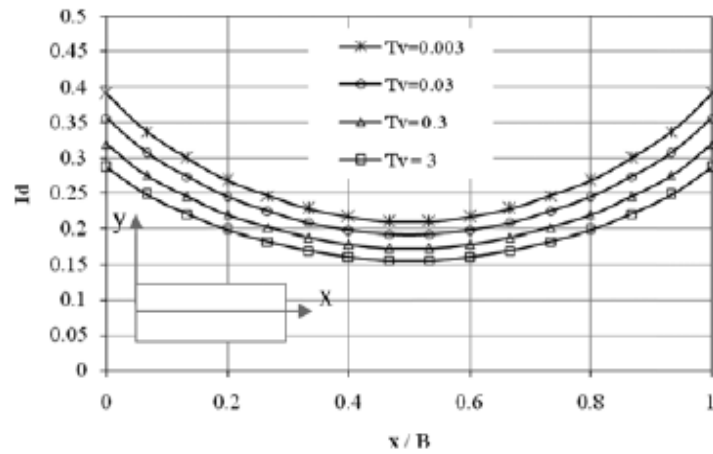


Fig. 10 Normalized vertical displacement under unpiled raft of (6×15) m size at different time factors

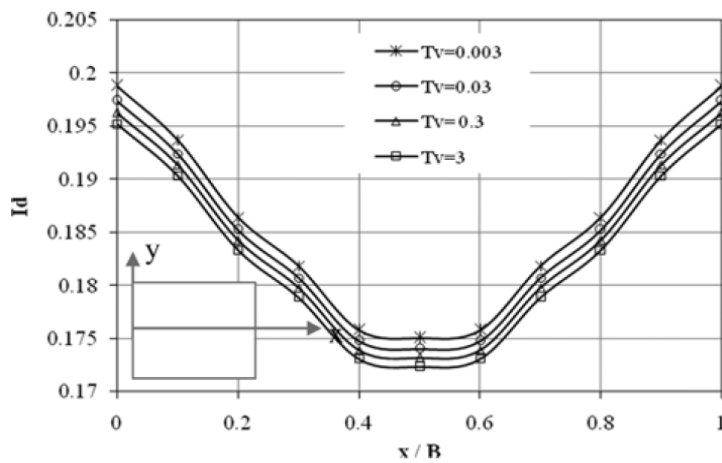


Fig. 11 Normalized vertical displacement under unpiled raft of (10×10) m size at different time factors

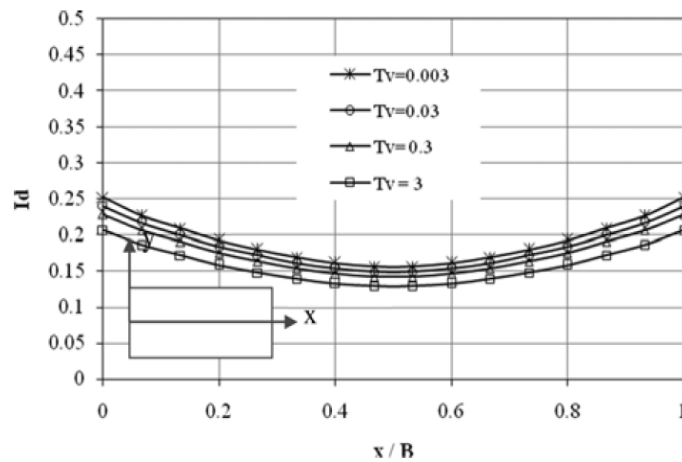


Fig. 12 Normalized vertical displacement under unpiled raft of (10×15) m size at different time factors

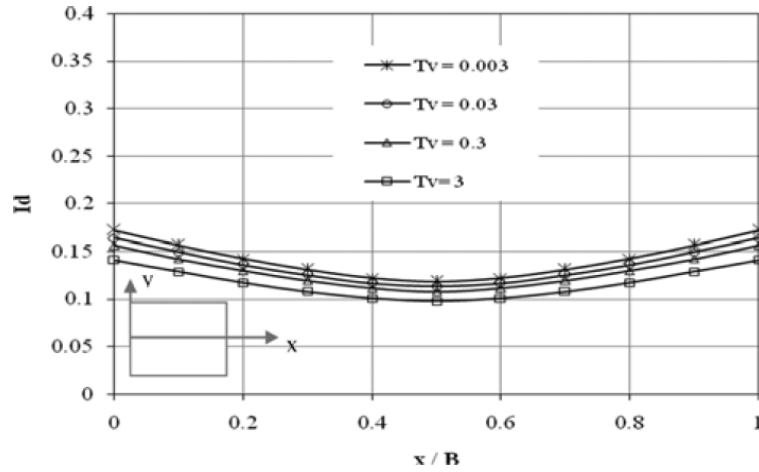


Fig. 13 Normalized vertical displacement under unpiled raft of (15×15) m size at different time factors

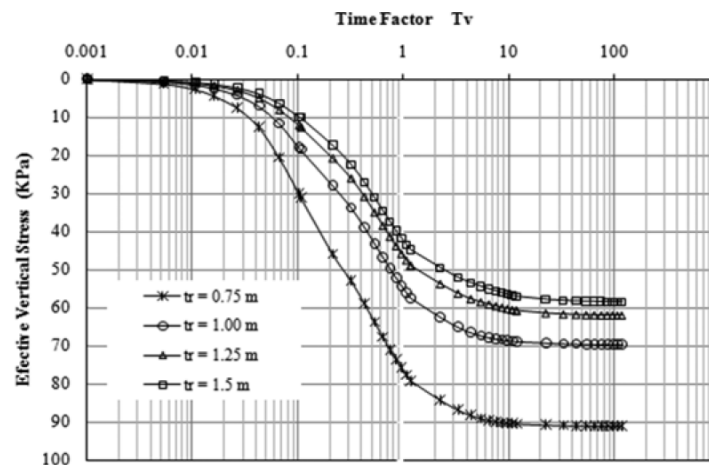


Fig. 14 Variation of vertical stress under the raft center with time for unpiled raft of (10×10) m for different thicknesses under a vertical load of 10000 kN

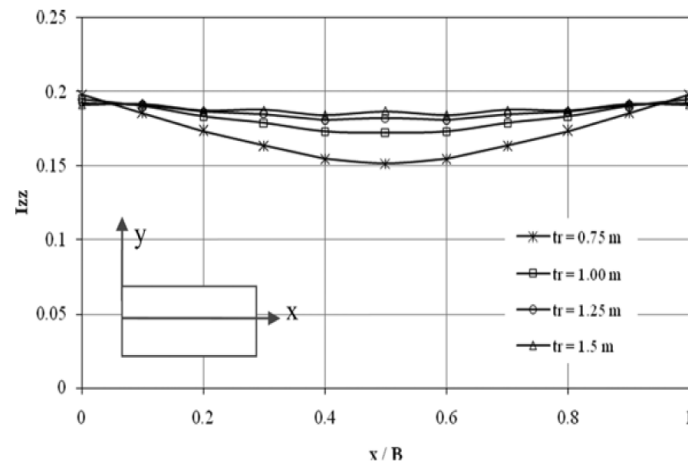


Fig. 15 Normalized displacement along the unpiled raft of (10×10) m for different thicknesses

pronounced in the case of 0.75 m raft thickness, where the settlement at the center is about 15% more than the other cases.

The bending moment along a vertical section passing through the center of the unpiled raft can be presented in the normalized form

$$I_M = \frac{M_x}{PB} \quad (3)$$

where,

- I_M = Normalized moment per unit length in the raft,
- M_x = Moment in the raft along the x-direction,
- B = Width of the raft measured in the x-direction, and
- P = Applied vertical load.

Fig. 16 shows the normalized moment at the centerline of the unpiled raft of size (10×10 m) for different thicknesses. The moment under the load is of maximum values for the four thicknesses, the change in moment is more pronounced at the raft edges where the moment at the edges of the unpiled raft 0.75 m thickness is about 80% greater than that of the unpiled raft with thickness of 0.75 m.

6. Time dependent behavior of the piled raft foundation

Five configurations of piled raft are studied herein; (2×1, 3×1, 2×2, 3×2 and 3×3) with raft dimensions of (6×10, 6×15, 10×10, 10×15 and 15×15) m, respectively. Lengths of piles, diameters of piles, spacing between piles, and thickness of the raft are kept constants with the values 20 m, 1.0 m, 5D, and 1.0 m, respectively. Piles in these groups are arranged symmetrically with square sections equivalent to those of circular cross section.

Figs. 17 to 21 present the pore water pressure variation with time for the five cases of group of piles under a vertical load of 10000 kN, the load is applied gradually and kept constant for all the groups to observe the change in pore pressure and displacement under the raft for these cases. The upper boundary of the soil model is considered as permeable boundary while the raft is impermeable footing. The case of (2×1) still maintain some pore pressure even after 50 months, but with value much lower than the respective case of unpiled raft. For the other cases, it was found that 50 months is enough time to allow the pore pressure under the raft to dissipate completely. Under the pile end, the pore pressures are generated with notable values as shown in the two dimensional plot for pore pressure with depth.

As shown in Fig. 18, for the case of (3×1) piled raft the pore water pressure under the raft has a value of 63% less than the maximum resulted from the applied load after 15 days, this value reduces to 85% of its maximum after one month. After 10 months, the value of pore pressure under the raft approximately vanishes. Under the center pile base, pore water pressure is also generated with a value about 50% of the maximum value of pore pressure that generates under the raft. This pressure is merged with the pressure generated under the raft and disappeared completely after 5 months.

The maximum pore water pressure generated under the piled raft of (2×2) configuration is about 22% less than that under the piled raft of (3×1) under the same applied load (Fig. 19), 84% of this pressure dissipates after 5 months, while the remaining may be reduced to a neglected value after 10 months.

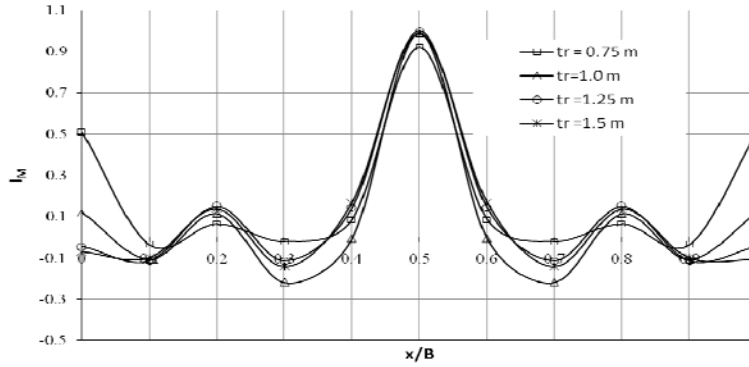
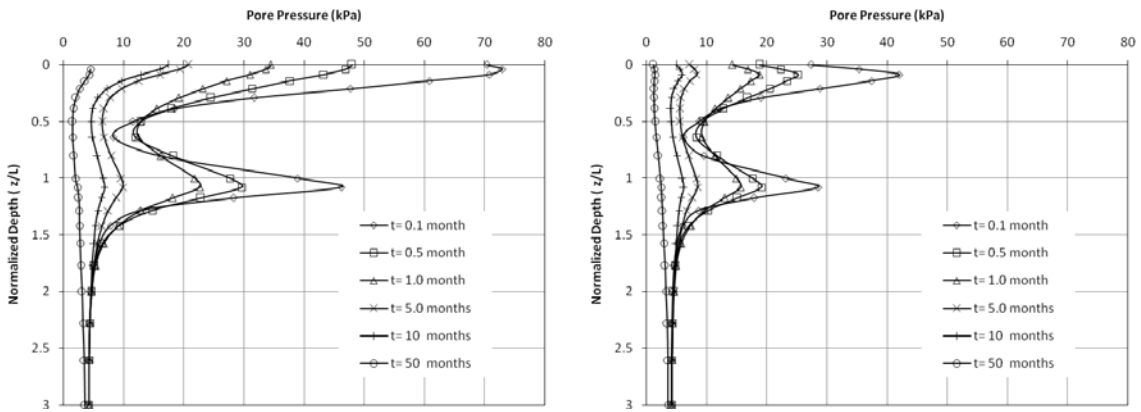


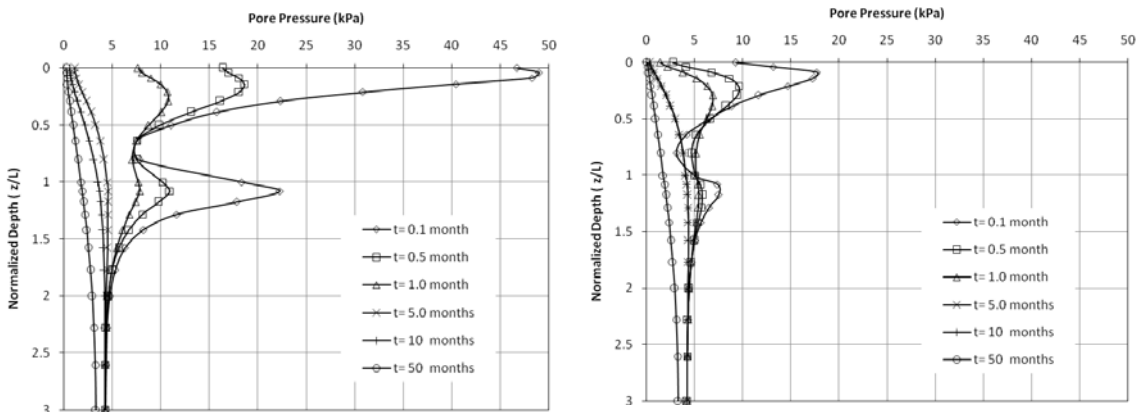
Fig. 16 Normalized displacement along the unpiled raft of (10×10 m) for different thicknesses



(a) Pore water pressure below the raft center at different times

(b) Pore water pressure below the raft edge at different times

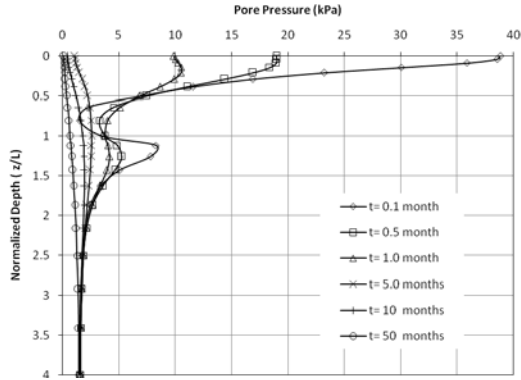
Fig. 17 Variation of pore water pressure beneath piled raft of (2×1) group



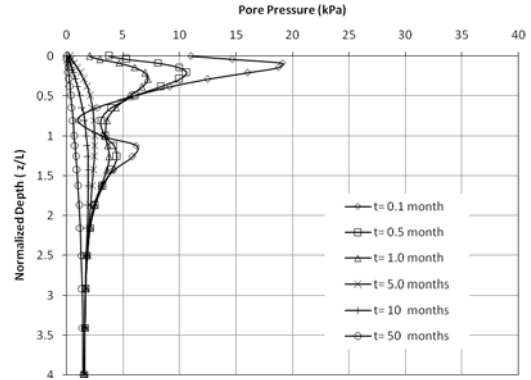
(a) Pore water pressure below the raft center at different times

(b) Pore water pressure below the raft edge at different times

Fig. 18 Variation of pore water pressure beneath piled raft of (3×1) group

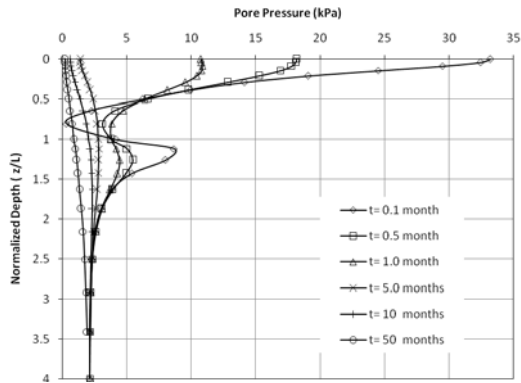


(a) Pore water pressure below the raft center at different times

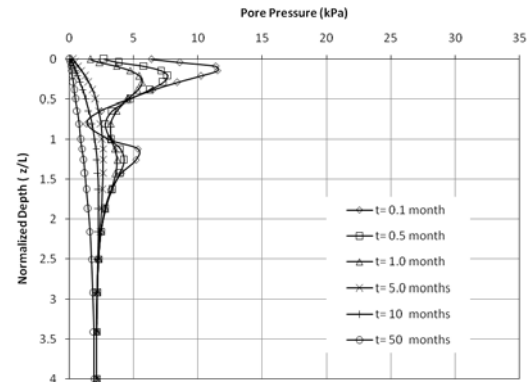


(b) Pore water pressure below the raft edge at different times

Fig. 19 Variation of pore water pressure beneath piled raft of (2x2) group

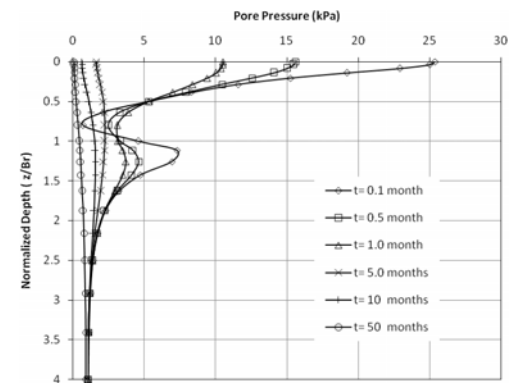


(a) Pore water pressure below the raft center at different times

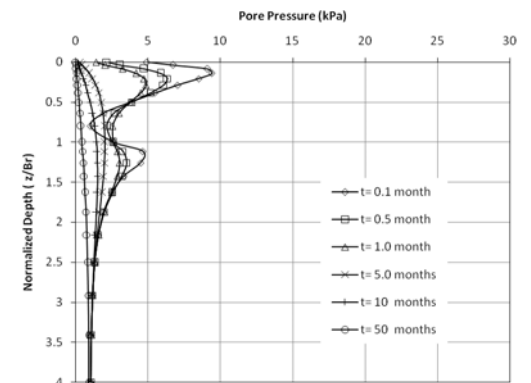


(b) Pore water pressure below the raft edge at different times

Fig. 20 Variation of pore water pressure beneath piled raft of (3x2) group



(a) Pore water pressure below the raft center at different times



(b) Pore water pressure below the raft edge at different times

Fig. 21 Variation of pore water pressure beneath piled raft of (3x3) group

The difference between the maximum pore water pressure under the piled rafts of (2×2) and (3×2) configurations is about 15%, which results from the wider area of the raft and greater number of piles of the group (3×2).

The biggest tested group with 9 piles was arranged as (3×3) with raft of (15×15 m) size. This group recorded the lowest maximum pore water pressure under the raft with value of (25.38 kPa) which is about 24% and 49% of the pressure under the piled raft of (3×2) and (3×1) respectively, as shown in Fig. 21.

The normalization factor presented in Eq. (1) is used for expressing the displacement of the raft in the vertical direction, the diameter of the pile is included in this factor instead of the raft thickness, as shown in Eq. (4). The dimensionless time factor presented in Eq. (2) is used to express the time.

$$I_z = \frac{PD}{u_z E_s BW} \quad (4)$$

where, D is the pile diameter.

Since only quarter of the piled raft problem is modeled in the finite element mesh, the displacement of the raft is shown only for one half. Figs. 22 to 26 show the normalized displacement of the raft at different times for the five groups of piles adopted in this study. The same vertical load is applied instantaneously to all cases, for a pile length to diameter ratio of 20, spacing to diameter ratio of 5, raft thickness of 1 m. It can be noticed that the differential displacement between the center and the edge of the raft is of maximum value for the groups of (3×1 and 3×2) where the raft is of rectangular geometry, for the other square section rafts (2×2 and 3×3) and the rectangular short section group of (2×1), the differential displacements are less than other cases.

The distribution of load along the pile may indicate the percent of load carried by piles to the total applied load. Figs. 27 to 31 show the percent of load carried by each pile and the total load of piles for the set of five piled rafts studied herein under concentrated vertical load applied at the center of the raft. The spacing to diameter ratio, pile diameter, pile length, thickness of the raft are kept constant at the values 5, 1.0 m, 20 m, and 1.0 m, respectively.

For the case of (2×1) piled raft, each of the two piles carry the same amount of load since the load is concentrated and applied at the center. It can be noticed that the force taken by the piles reduces as moving from the head to the base of the pile and this is normal since the skin friction is of maximum value near the pile head.

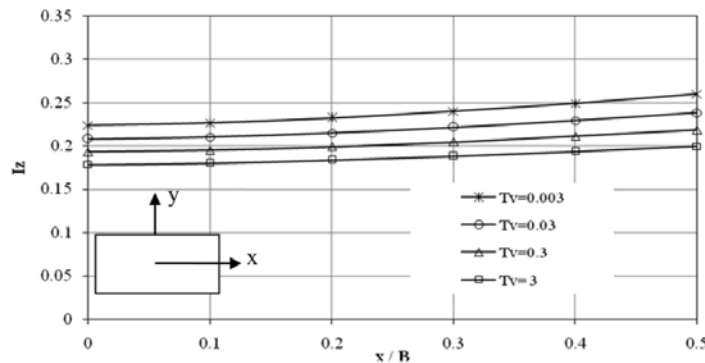


Fig. 22 Normalized vertical displacement under piled raft of (2×1) group at different time factors

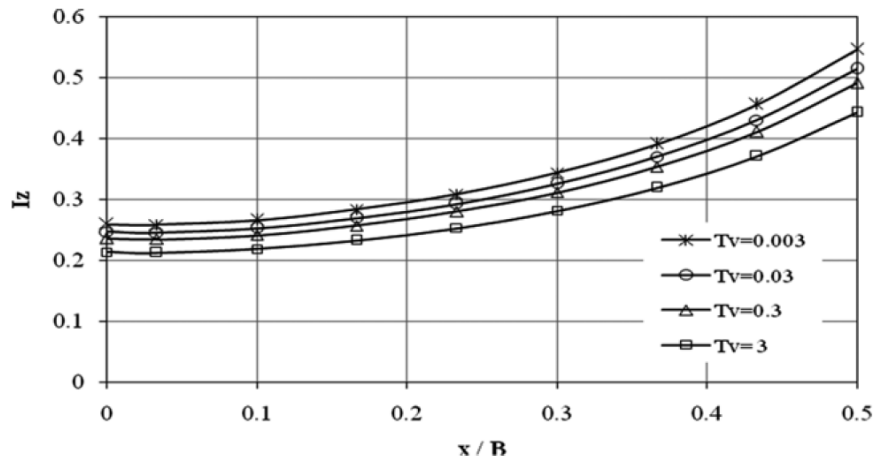


Fig. 23 Normalized vertical displacement under piled raft of (3x1) group at different time factors

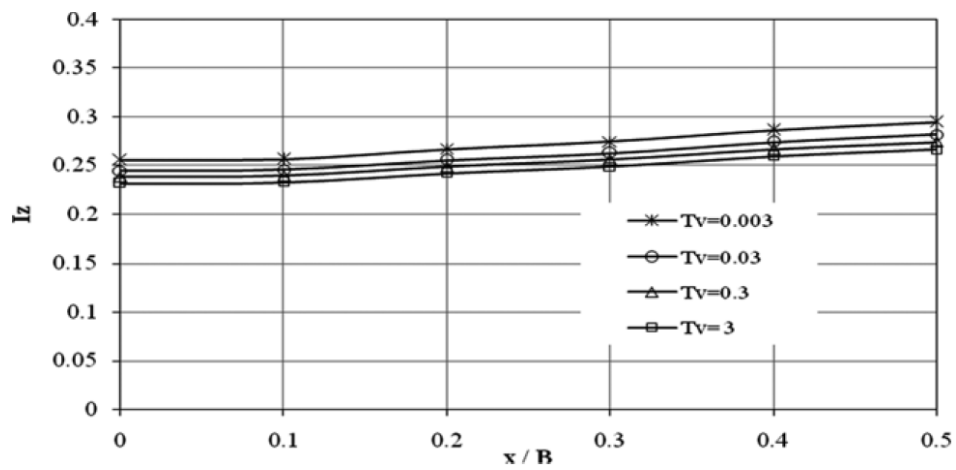


Fig. 24 Normalized vertical displacement under piled raft of (2x2) group at different time factors

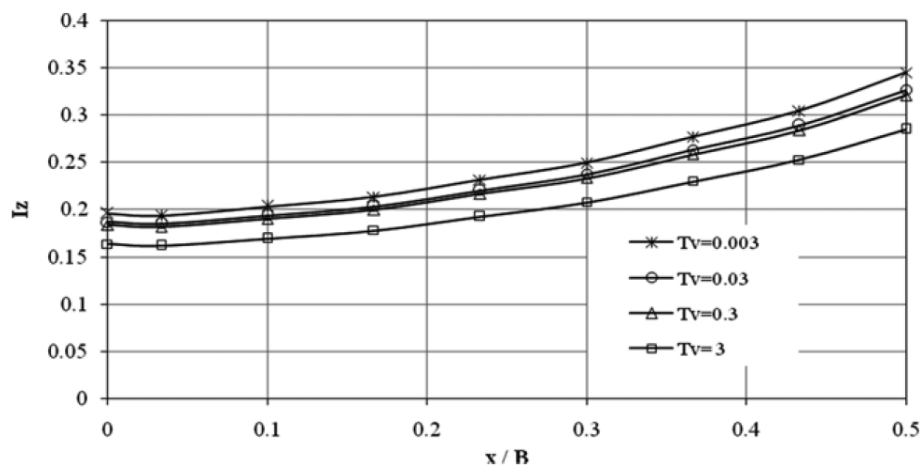


Fig. 25 Normalized vertical displacement under piled raft of (3x2) group at different time factors

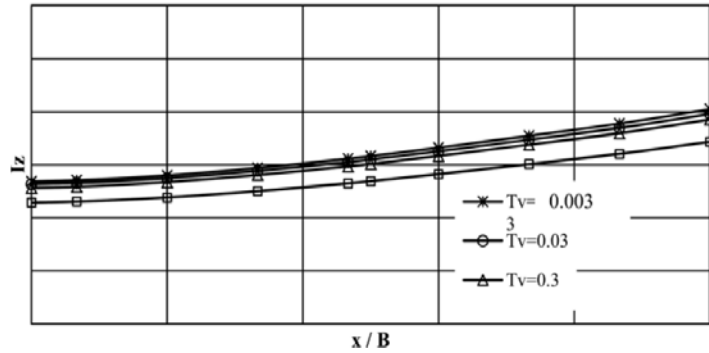


Fig. 26 Normalized vertical displacement under piled raft of (3x3) group at different time factors

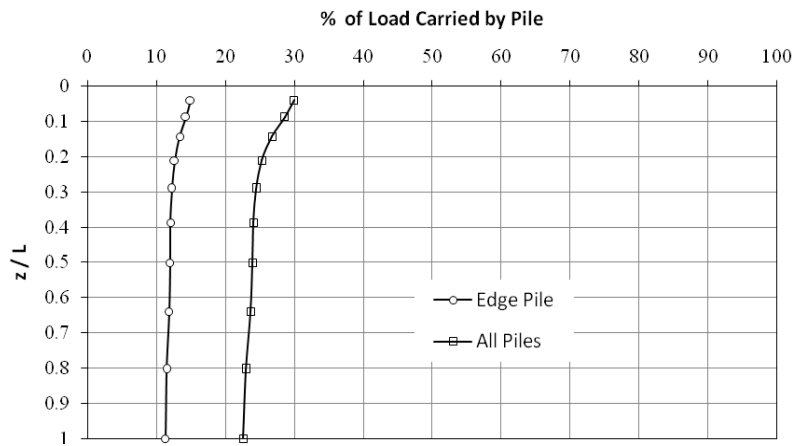


Fig. 27 Variation of the percent of load carried by piles with depth for (2x1) piled raft, at the end of consolidation

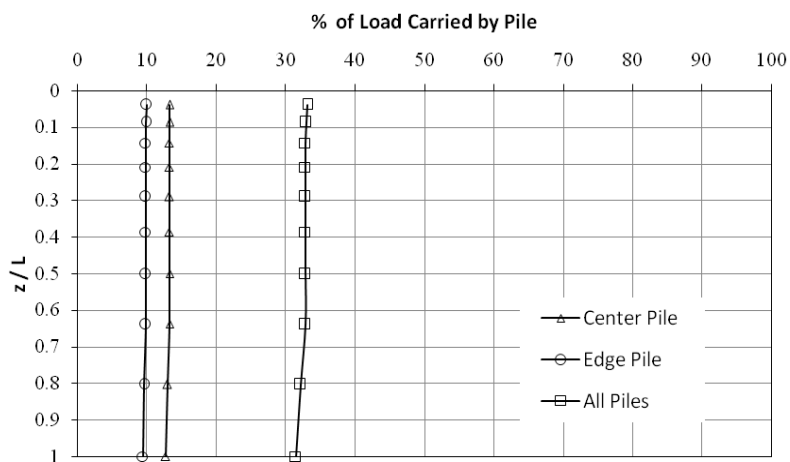


Fig. 28 Variation of the percent of load carried by piles with depth for (3x1) piled raft, at the end of consolidation

For the case of (3×1) piled raft, in addition to the raft, there are three piles to share the load. Due to symmetry, the edge piles have the same share of load while the center pile carries load about 1.35 times the load carried by the edge pile.

The total load carried by piles in the (2×2) group can be found by multiplying the load carried by one pile by (4) making use of the symmetry and the loading condition. The average load carried by piles is about 42% of the total load where each pile carries 10.5% of the total applied load.

In the case of (3×2) piled raft, there are two piles considered as center piles and the other four as corner piles, each one of the center piles is noticed to carry an average load of about 1.25 of the average load carried by the corner pile, and the total load carried by all piles was found to be 62% of the total applied load.

For the case of (3×3) piled raft, the behavior of piles can be categorized into three types; center pile, edge pile, and corner pile, where the load distribution along each of these piles is different as shown in Fig. 31. The average percent of load taken by center pile is about 12% which is equal to 1.285 times the percent of load taken by the edge pile and 1.5 times the percent of load taken by the corner pile. The edge pile takes load of about 1.15 of load taken by the corner pile. These different percents of load carried by pile may result from the relatively large spacing to diameter ratio which reduced the interaction between piles.

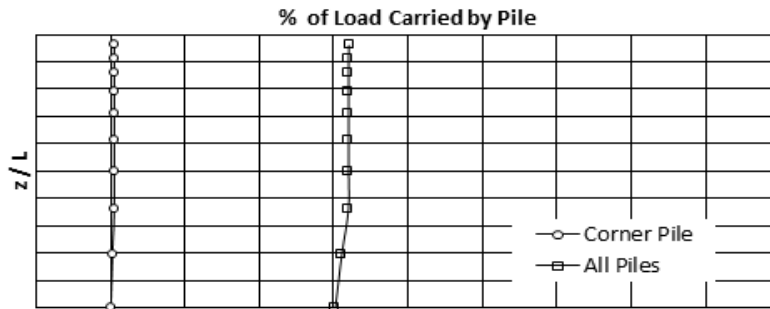


Fig. 29 Variation of the percent of load carried by piles with depth for (2×2) piled raft, at the end of consolidation

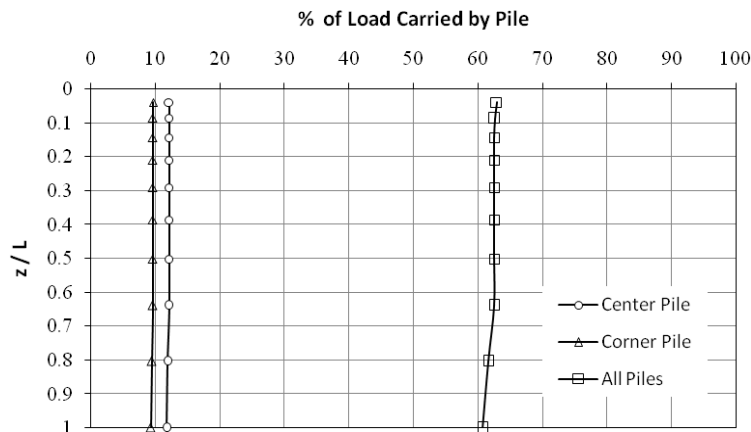


Fig. 30 Variation of the percent of load carried by piles with depth for (3×2) piled raft, at the end of consolidation

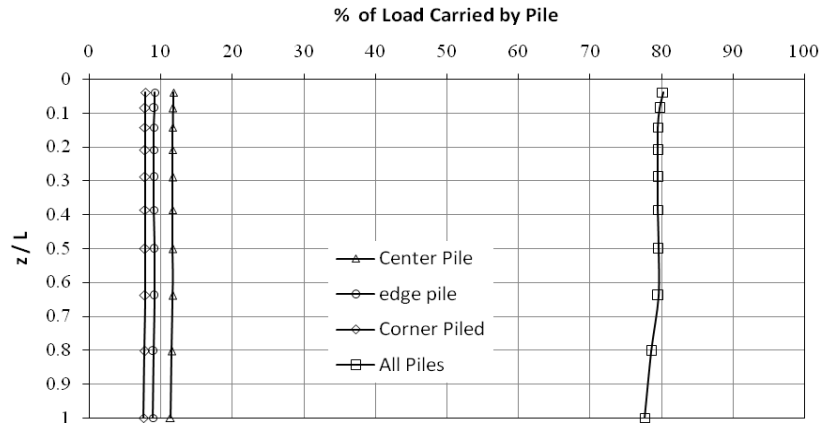


Fig. 31 Variation of the percent of load carried by piles with depth for (3×3) piled raft, at the end of consolidation

7. Conclusions

In comparison to shallow (raft) foundations, piled rafts reduce effectively the settlements, the differential settlements and the bending moment in the raft proportionally. The time-dependent behavior of the soil originated by consolidation has obvious effects on the whole interaction system of pile-raft-soil. The characteristics of time variation of excess pore water pressure in the soil are intimately associated with geometry of the raft including its width and thickness.

Settlement beneath the piled raft foundation resulted from the dissipation of excess pore water pressure considerably affects the final settlement of the foundation, and enough attention should be paid to settlement variation with time. The settlement behavior of unpiled raft shows bowl shaped settlement profile with maximum at the center. The degree of curvature of the raft under vertical load increases with the decrease of the raft thickness. For the same vertical load, the differential settlement of raft of (10×10 m) size decreases by more than 90% when the raft thickness increased from 0.75 m to 1.5 m.

The average load carried by piles depends on the number of piles in the group. The groups of (2×1, 3×1, 2×2, 3×2, and 3×3) piles were found to carry about 24%, 32%, 42%, 58%, and 79% of the total vertical load. The distribution of load between piles becomes more uniform with the increase of raft thickness. For an unpiled raft with high stiffness, the pile may share the same amount of load. The moment under the load is of maximum values for all values of raft thickness, the change in moment is more pronounced at the raft edges where the moment at the edges of the unpiled raft 0.75 m thickness is about 80% greater than that of the unpiled raft with thickness of 0.75 m.

References

- ABAQUS Theory Manual, version, (2008), Hibbitt, Karlsson & Sorenson, Inc.
 Al- Saady, N.H. (1989), "Analysis of an A-6 soil during construction of a road embankment", M.Sc. thesis,

- University of Baghdad, Iraq.
- Al-Zayadi, A.A.O. (2010), "Three-dimensional analysis of piled-raft foundation", Ph.D. Thesis, University of Baghdad, Iraq.
- Chow H. (2007), "Analysis of piled-raft foundation with piles of different lengths and diameters", Ph.D. Thesis, School of Civil Engineering, the University of Sydney.
- Russo, G. and Viggiani, C. (1998), "Factors controlling soil-structure interaction for piled Rafts", *Darmstadt Geotechnics, Darmstadt University of Technology*, **4**, 297-322.
- Small, J.C. and Liu, L.S. (2008), "Time-settlement behaviour of piled raft foundations using infinite elements", *Comput. Geotech.*, **35**, 187–195.

GM